Experimental Test Bench of Photovoltaic Panel Under Partial Shading Effect Using the SLG-Backstepping Technique

Mohammed Ferfra*, Mohcine Mokhlis*‡, Khalid Chennoufi*

* Department of Electrical Engineering, Mohammadia School of Engineers, Mohammed V University in Rabat, Ibn Sina Street P.B 765, Rabat

(mohcine1mo@gmail.com, mohaferfra@gmail.com, chennoufi.khalid@gmail.com)

‡ Corresponding Author; Mohcine Mokhlis, Tel: +212 628 984 358, mohcine1mo@gmail.com

Received: 10.03.2021 Accepted:21.04.2021

Abstract- Under the partial shading effect, the Power-Voltage curve of a photovoltaic panel includes several maximum power points divided between the local maximums and a global maximum. The most known Maximum Power Point Tracking techniques are unable to distinguish the global maximum power point. Thus, they result in a considerable drop in power. In fact, the Global Maximum Power Point Tracking technique based on the SLG-Backstepping command strategy is able to distinguish and track the global maximum power point. In the previous works, this command strategy has proven its tracking performances (accuracy and rapidity) when it is tested under Matlab/Simulink environment. In this work, this paper focuses on the real-time experimental assessment of the newest SLG-Backstepping command strategy, these tests are carried out in order to prove the ability of this command strategy to provide the desired performances, to detect any change of meteorological conditions and to track the global maximum in the real time. This strategy command is compared to the Maximum Power Point Tracking technique based on the P&O-Backstepping command strategy. In fact, these two controllers are implemented on the Arduino Mega 2560 board. Effectively, according to the experimental results, the SLG-Backstepping command strategy is able to detect the presence of partial shading and to track the global maximum under the partial shading effect. In addition, this strategy command shows tracking performances better than the P&O-Backstepping controller when they are compared under uniform meteorological conditions. In fact, as affirm results, the proposed command strategy tracks the maximum power point in approximately 0.7s, while the MPPT technique based on the P&O-Backstepping make a delay of 1.5s, also, also, under the partial shading effect, a considerable loss of power is noticed when using the MPPT technique.

Keywords Arduino Mega 2560 Board, Backstepping technique, BOOST converter, Global Maximum Power Point Tracking technique, Partial shading effect, SLG algorithm.

Nomenclature

C_{pv}	:	Capacitance of the input capacitor (μF).
C_{out}	:	Capacitance of the output capacitor (μF).
$\varepsilon_1, \varepsilon_2$	:	Tracking errors.
I_{pv}	:	Photovoltaic current (A).
I_L	:	Inductor current (A).
I_{out}	:	Output current (A).
α	:	Virtual control.
K_1, K_2	:	Positive constants (control parameters).
V_{pv}	:	Photovoltaic Voltage (V).
V_{out}	:	Output Voltage (V).
V_{ref}	:	Reference Voltage (V).
$P_{\max\_load}$	:	Maximal power dissipation.
P_{pv}	:	Photovoltaic maximum (W).
L	:	Inductance of the Boost inductor (mH).

d	:	Duty cycle (control law).
MPPT	:	Maximum Power Point Tracking.
GMPPT	:	Global Maximum Power Point Tracking.
LMPP	:	Local Maximum Power Point.
GMPP	:	Global Maximum Power Point.
SLG	:	Sweep, Look and Generate algorithm.
P&O	:	Perturb and Observe algorithm.
InC	:	Incremental Conductance.
PV	:	Photovoltaic.
$V_1(\varepsilon_1)$, $V_2(\varepsilon_1, \varepsilon_2)$	:	Lyapunov functions.
DC	:	Direct-Current.

1. Introduction

Photovoltaic resources have become in demand thanks to their simplicity of installation and maintenance, non-exhaustion and cleanliness [2]-[3]. Also, this kind of the renewable energies can be installed close to the consumer, which reduces the cost of transporting energy and power losses. However, the efficiency of these resources is highly dependent on the weather conditions [4]-[5].

To improve efficiency of the photovoltaic energy, it must operate the photovoltaic panels at the maximum power point taking into account the weather conditions' changes. To reach this goal, researchers are proposing the Maximum Power Point Tracking technique. This technique can track the maximum power point when the ambient meteorological conditions are uniform.

The MPPT technique based on the P&O-Backstepping command strategy is designed in [6] in order to improve the tracking performances of the classical algorithms P&O [7]-[8]-[9] and InC [10]-[11]). The P&O-Backstepping command strategy includes two controllers, the P&O algorithm and a nonlinear command based on the Backstepping controller. The P&O algorithm is used to generate the reference trajectory that carries the optimal voltage value while the Backstepping controller is designed in order to follow that reference trajectory by adjusting the duty cycle of the BOOST converter.

In fact, although the P&O-Backstepping command strategy proposes good tracking performances under the normal meteorological conditions, it remains unable to operate efficiently under the partial shading effect, because in this case, the Power-Voltage curve (P-V) presents several maximum power points divided between the Local Maximum Power Points (LMPPs) and one Global Maximum Power Point (GMPP)) [12]-[13]. Indeed, MPPT techniques can not distinguish the global maximum power point. Thus, they lead to a sharp drop in power in certain cases of partial shading.

To remedy the partial shading effect, a new algorithm called SLG is proposed in [2]-[14], this algorithm allows the scanning of the PV characteristic followed by the search for the maximum power point. Here, the sliding mode controller is used in order to allow the PV voltage to pursue a voltage reference trajectory, which is returned by the SLG algorithm, by adjusting the Sepic converter's duty cycle.

This paper offers the experimental test bench of two photovoltaic modules subjected to the partial shading effect and controlled by the SLG-backstepping command strategy. Indeed, this latter is implemented on the Arduino Mega 2560 Board that serves to generate the PWM signal, which is dedicated to controlling the Boost converter's transistor. The second aim is to show the criteria's performances of the proposed technique compared to the P&O-Backstepping command strategy under the uniform meteorological conditions. The proposed system is composed of a BOOST converter, a DC load (Resistive load of 50Ω), and two photovoltaic modules (Reference: SP20-36P) of Maximal power of 20W.

In fact, the main objectives of this paper are summarized in the following lines:

- Providing the experimental test bench of the proposed SLG-Backstepping controller.
- Testing the performances of the proposed controller under uniform and nonuniform meteorological conditions (partial shading effect).
- Comparing the proposed controller with the MPPT technique (P&O-Backstepping) in terms of tracking performance and power production.

This article is organized as follows, section 2 presents the proposed photovoltaic system, section 3 covers the details of the proposed command strategy. Section 4 is devoted to the discussion of the experimental results, while the last section is dedicated to the conclusion.

2. Studied Photovoltaic System

The studied PV system consists of three essential components:

- Photovoltaic panel composed of two PV modules (Reference: SP20-36P) connected in series, which means that the maximal power can produce this photovoltaic source is 40W, which is equal to 20W×2. The electrical characteristic of the SP20-36P photovoltaic module is listed in Table 1.
- Boost converter, its parameters are listed in Table 2. As depicted Fig.2b, two inductors are connected in series to obtain the equivalent inductor of approximately 0.66mH, and four output capacitors are connected in series to obtain an equivalent capacitor of approximately 220µF.
- Resistive load (Resistance of 50Ω with a maximal power dissipation of 100W).

The Arduino Mega 2560 Board is programmed, using the proposed SLG-Backstepping command strategy, in order to generate the PWM signal that can control the BOOST converter's MOSFET. The studied PV system is illustrated in Fig.1, while the technical specifications of the studied Arduino are listed in Table 3.

Table 1. Electrical characteristics of the studied PV modules (Reference: SP20-36P)

Parameters	Values
Maximal power (P_{max})	$20W$
Optimal voltage (V_{opt})	$17.3V$
Optimal current (I_{opt})	$1.16A$
Open-circuit voltage (V_{oc})	$21.7V$
Short-circuit current (I_{sc})	$1.26A$

Table 2. Electrical characteristics of the designed BOOST converter.

Parameters		**Values**
Inductance L		$0.66mH$
Input capacitance (C_{pv})		$470\mu F$
Output capacitance (C_{out})		$220\mu F$
Maximal input voltage (V_{PV})		$63V$
Maximal output voltage (V_{out})		$400V$
Switching frequency (Khz)		$32Khz$
Mosfet IRFZ44N	Maximum Continuous source current (I_S)	$49A$
	Diode Forward Voltage (V_{SD})	$1.3V$
	Minimum Drain-to-Source Breakdown Voltage (V_{SDD})	$55V$
Schottky Diode SR540	DC Blocking Voltage	$40V$
	Forward Voltage for a Forward current $I_F = 5A$	$0.55V$

Table 3. Electrical specifications of the Arduino Mega 2560 board.

Microcontroller	ATmega2560
Operating Voltage	$5V$
Input Voltage (recommended)	$7-12V$
Input Voltage (limits)	$6-20V$
Digital I/O Pins	54 (of which 14 provide PWM output)
Analog Input Pins	16
DC Current per I/O Pin	$40mA$
DC Current for 3.3V Pin	$50mA$
Flash Memory	$256KB$ of which $8KB$ used by bootloader
SRAM	$8KB$
EEPROM	$4KB$
Clock Speed	$16Mhz$

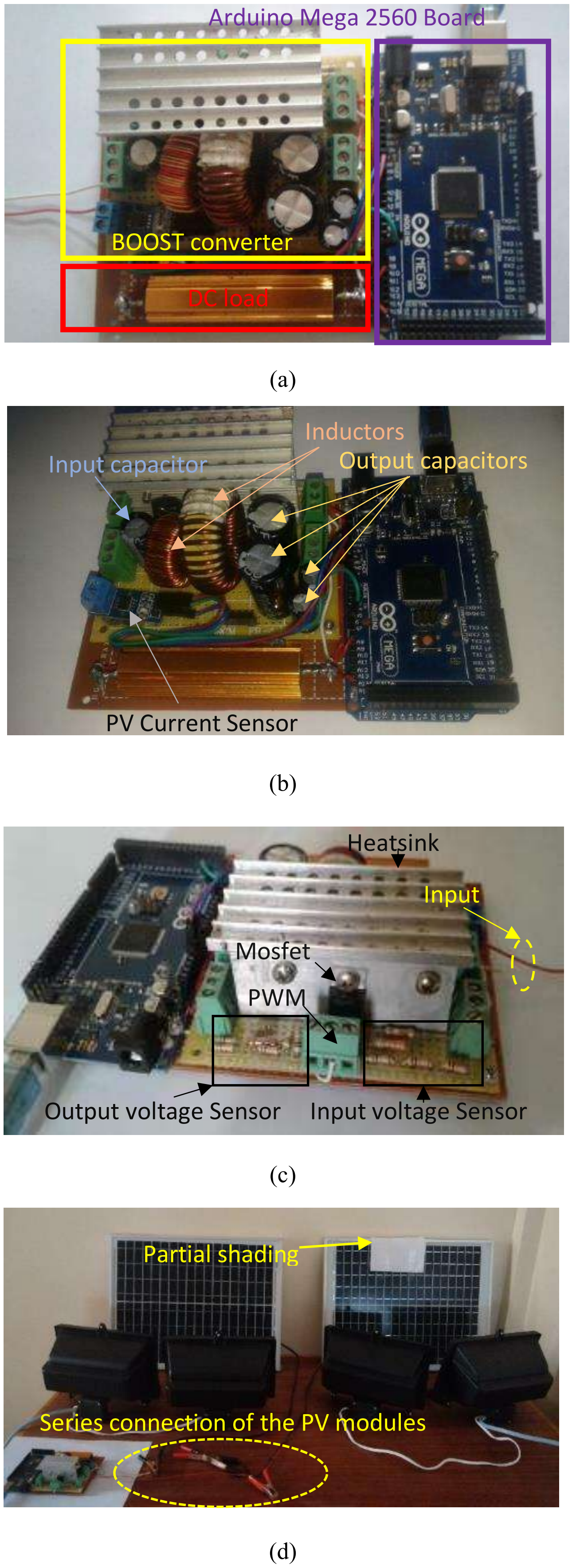

Fig. 1. Hardware Implementation: a – Top view, b – Right side view, c – Left side view, d - Experimental Test bench.

2.1. State equation of the Boost converter

The modelling of the Boost converter passes through studying two switching phases, (as detailed in [12]). Also, by using the average value method [15], the following state equation can be obtained:

$$\begin{cases} \dfrac{dV_{PV}}{dt} = \dfrac{1}{C_{PV}} I_{PV} - \dfrac{1}{C_{PV}} I_L \\ \dfrac{dI_L}{dt} = \dfrac{1}{L} \mathrm{V}_{PV} - \dfrac{1}{L}(1-\mathrm{d})V_{out} \\ \dfrac{dV_{out}}{dt} = \dfrac{1}{C_{out}}(1-\mathrm{d})I_L - \dfrac{1}{C_{out}} I_{out} \end{cases} \tag{1}$$

2.2. Current and voltage sensors

The current sensor used, (see Fig.2), is the ACS712. This sensor can measure a maximum current of 30A and has a sensitivity of 66mV/A.

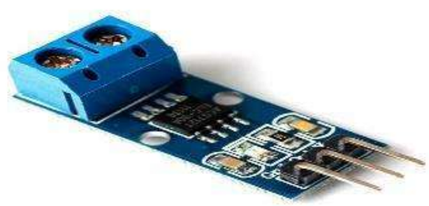

Fig. 2. ACS712 current sensor.

The input voltage sensor, that is designed, (see Fig.3), can support a maximal input voltage of $50.45V$ that is equal to $5V \times (9.83k\Omega + 89.37k\Omega)/9.83k\Omega$, which is more enough in this study. Because, the maximal voltage, that can produce two PV modules (Reference: SP20-36P) connected in series, does not exceed $43.4V$, "$2 \times V_{oc}$".

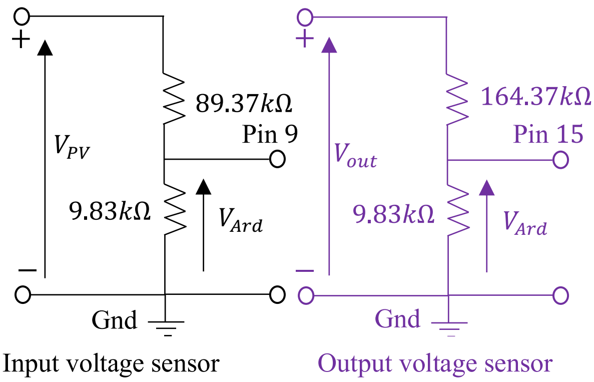

Fig. 3. Voltage sensors (voltage dividers).

The output voltage sensor, (see Fig.3), is designed to be able to measure a maximal voltage of $88.6V$ "$5V \times (9.83k\Omega + 164.3k\Omega)/9.83k\Omega$".

3. Control Design

To overcome the issue of the power losses that is due to the partial shading effect, the SLG-Backstepping is proposed. This hybrid technique is composed of two loops, the first one is the SLG algorithm, while the other one is the nonlinear controller based on the Backstepping command. Actually, the SLG algorithm sweeps the P-V curve of the PV modules each time when there is a detection of the partial shading. Also, in the same time, this algorithm looks for the GMPP, then, it generates the corresponding optimal voltage as a reference trajectory to be tracked by the Backstepping command. In fact, the SLG algorithm stops scanning the P-V curve whenever the PV voltage is close to reaching the value of the open circuit voltage. The flowchart of the proposed SLG-Backstepping command strategy is shown in Fig.4, [2]- [14].

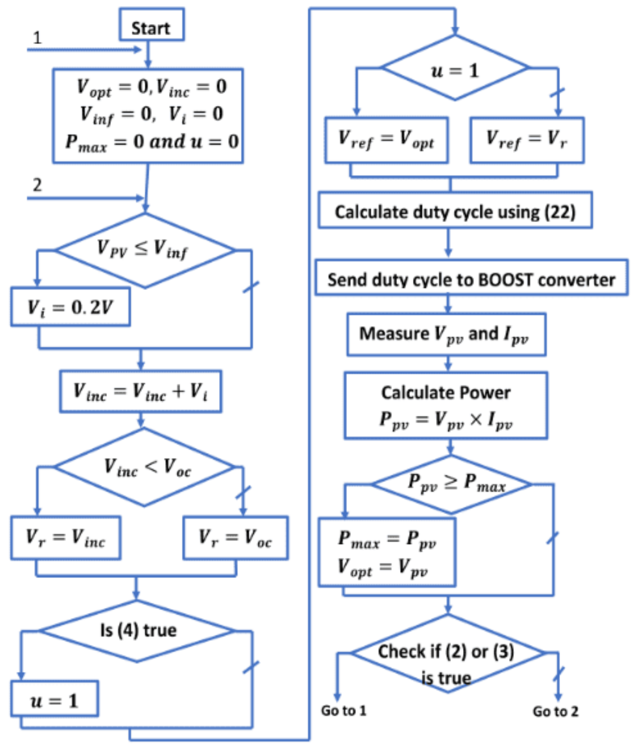

Fig. 4. Flowchart of the proposed SLG-Backstepping algorithm.

- The partial shading is detected when one of the following conditions is true :

$$\begin{cases} V_{PV} - V_{opt} \le -\Delta V \\ P_{PV} - P_{max} \le -\Delta P \end{cases} \tag{2}$$

$$P_{PV} - P_{max} \ge \Delta P \tag{3}$$

with
ΔV and ΔP is the detection thresholds.

- The SLG algorithm stops scanning the P-V curve when the following condition is true :

$$\begin{cases} V_{pv} \geq V_c \\ P_{pv} \leq P_c \end{cases} \tag{4}$$

with

V_c : Constant variable supposed equal *17V*.
P_c : Constant variable supposed equal *5W*.

3.1. Backstepping command

The Backstepping command is a nonlinear controller that is devoted especially to the nonlinear systems, this command allows the PV system to be more performant [17]. The designing steps of this command are as follows:

- Step 1:

For designing the Backstepping command, it must define the output y and the reference trajectory y_{ref}. Knowing that this technique allows the PV voltage to pursue the voltage reference generated by the SLG algorithm. Therefore, in this case, the output is $y = V_{pv}$ while the output reference is $y_{ref} = V_{ref}$.

The tracking error is defined by the following expression:

$$\varepsilon_1 = y - y_{ref} = V_{PV} - V_{ref} \tag{5}$$

The time derivative of ε_1 is expressed as follows:

$$\dot{\varepsilon}_1 = \dot{V}_{PV} - \dot{V}_{ref} \tag{6}$$

Using (1) and (6) the following equation can be obtained:

$$\dot{\varepsilon}_1 = \frac{I_{PV} - I_L}{C_{PV}} - \dot{V}_{ref} \tag{7}$$

In order to ensure the Lyapunov stability, the time derivative of the following Lyapunov function has to be negative [18]-[19]:

$$V_1(\varepsilon_1) = \frac{1}{2}\varepsilon_1{}^2 \tag{8}$$

The time derivative of (8) is as follows:

$$\dot{V}_1(\varepsilon_1) = \varepsilon_1\dot{\varepsilon}_1 = \varepsilon_1\left(\frac{I_{PV} - I_L}{C_{PV}} - \dot{V}_{ref}\right) \tag{9}$$

Equation (9) must be negative. For this reason, $\dot{V}_1(\varepsilon_1)$ can also be expressed as follows:

$$\dot{V}_1(\varepsilon_1) = -K_1\varepsilon_1{}^2 < 0 \tag{10}$$

With K_1 is positive constant ($K_1 > 0$).

From equations (9) and (10), the following expression can be concluded:

$$\frac{I_{PV} - I_L}{C_{PV}} - \dot{V}_{ref} = -K_1\varepsilon_1 \tag{11}$$

Assuming a novel variable α that embodies the virtual control, with $\alpha = (I_L)_d$ and $(I_L)_d$ is the desired value of the state variable I_L. Therefore, referring to the equation (11), the virtual control α and its time derivative would be:

$$\alpha = -C_{PV}\dot{V}_{ref} + I_{PV} + C_{PV}K_1\varepsilon_1 \tag{12}$$

$$\dot{\alpha}_1 = -C_{PV}\ddot{V}_{ref} + \dot{I}_{PV} + C_{PV}K_1\dot{\varepsilon}_1 \tag{13}$$

- Step2:

Defining the novel tracking error and its time derivative as follows:

$$\varepsilon_2 = I_L - \alpha \tag{14}$$

$$\dot{\varepsilon}_2 = \dot{I}_L - \dot{\alpha} \tag{15}$$

Substituting the second equation of the state equation (1) in (15), the time derivative of ε_2 will be:

$$\dot{\varepsilon}_2 = \frac{1}{L}V_{PV} - \frac{1}{L}(1-d)V_{out} - \dot{\alpha} \tag{16}$$

The second Lyapunov function is expressed as follows:

$$V_2(\varepsilon_1, \varepsilon_2) = V_1(\varepsilon_1) + \frac{1}{2}\varepsilon_2{}^2 \tag{17}$$

Its time derivative would be:

$$\dot{V}_2(\varepsilon_1, \varepsilon_2) = \dot{V}_1(\varepsilon_1) + \varepsilon_2\dot{\varepsilon}_2 \tag{18}$$

Introducing (14), the new expression of the time derivative of the Lyapunov function $V_1(\varepsilon_1)$ (eq. (9)) can be obtained :

$$\dot{V}_1(\varepsilon_1) = -K_1\varepsilon_1{}^2 - \frac{\varepsilon_1\varepsilon_2}{C_{PV}} \tag{19}$$

Now, replacing equation (19) in equation (18), the following time derivative of $V_2(\varepsilon_1, \varepsilon_2)$ becomes as follows:

$$\dot{V}_2(\varepsilon_1, \varepsilon_2) = -K_1\varepsilon_1{}^2 + \varepsilon_2\left(-\frac{\varepsilon_1}{C_{PV}} + \dot{\varepsilon}_2\right) \tag{20}$$

To ensure that the time derivative of the Lyapunov function $V_2(\varepsilon_1, \varepsilon_2)$ is negative, the following expression must be validated:

$$-\frac{\varepsilon_1}{C_{PV}} + \dot{\varepsilon}_2 = -K_2\varepsilon_2 < 0 \tag{21}$$

With K_2 is a positive constant.

Replacing equation (16) in equation (21), the following control law is obtained:

$$d = 1 - \frac{L}{V_{out}}\left(-\frac{\varepsilon_1}{C_{PV}} + \frac{V_{PV}}{L} + K_2\varepsilon_2 - \dot{\alpha}\right) \tag{22}$$

With this choice

$$\dot{V}_2(\varepsilon_1,\varepsilon_2) = -K_1{\varepsilon_1}^2 - K_2{\varepsilon_2}^2 < 0 \qquad (23)$$

Therefore, this control law d ensures the asymptotic convergence of the errors ε_1 and ε_2 to 0. Thus, it ensures the convergence of V_{PV} to V_{ref}.

4. Experimental Results

In order to test the SLG-Backstepping command strategy in the real-time and under the partial shading effect, two PV modules (Reference: SP20-36P) are connected in series, and one of them is considered partially shaded as can be seen in Fig.1d.

Unlike the PV system, discussed in [2]-[14], which includes the SEPIC converter as an adaptation stage, and which is above all characterized by its filtering performance of the harmonics included in the currents and voltages better than the BOOST converter, this study focuses on the discussion of the performance of the proposed SLG-Backstepping technique in the real-time by comparing it with the existing MPPT technique based on the P&O-Backstepping and considering the Boost converter as the adaptation stage.

The PV modules, connected in series, can produce a maximal power of 40W under the standard conditions (irradiation of $1000W/m^2$ and a temperature of $25°C$). In this study, the PV modules are supposed subjected to a constant radiance coming from four spotlights used as can be seen in Fig.1d.

The MATLAB/Simulink environment is used for deploying the discussed techniques to the Arduino Mega 2560, as depicted Fig.5.

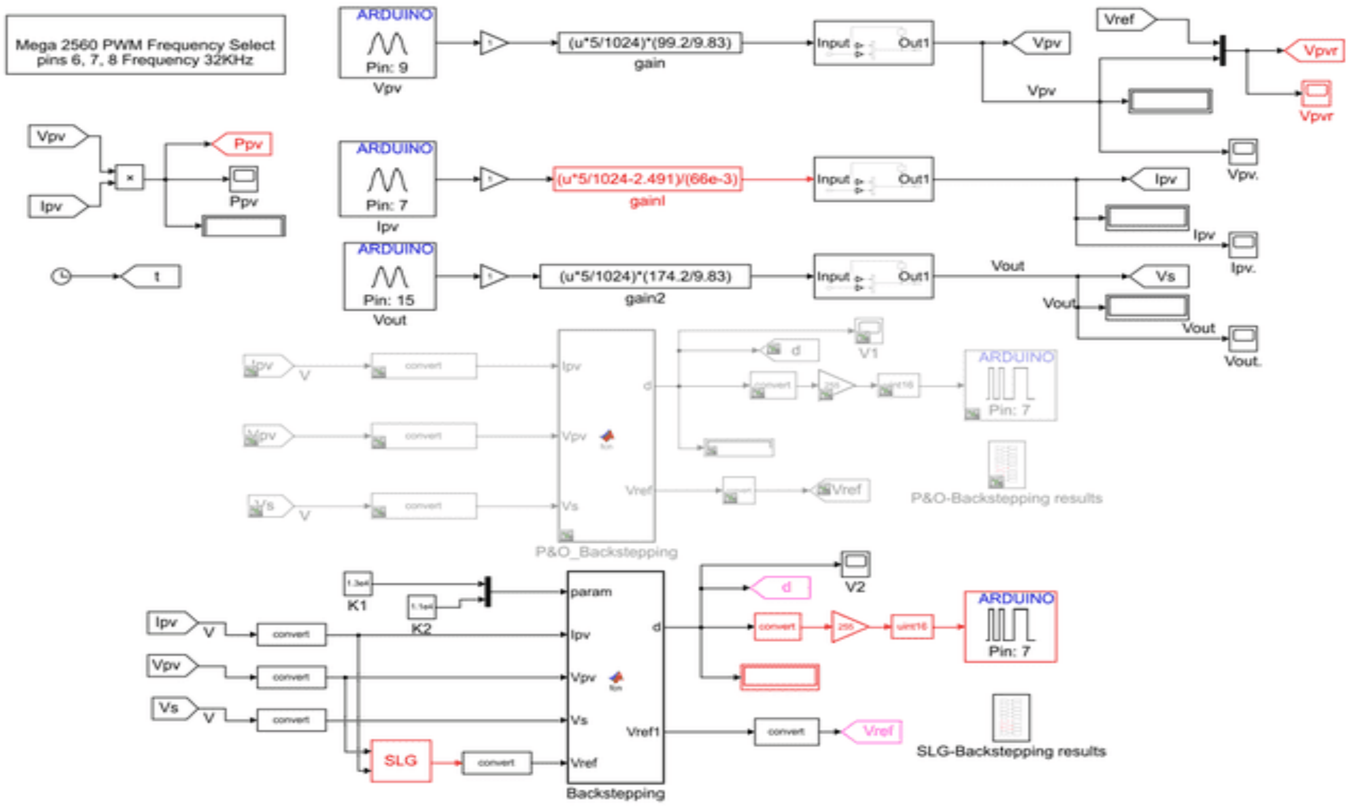

Fig. 5. Matlab/Simulink environment: Controllers to deploy on the Arduino board.

• P&O-Backstepping parameters:

$\Delta V_{P\&O} = 0.04V$, $K_1 = 1.3 \times 10^4$, $K_2 = 1.1 \times 10^4$.
With $\Delta V_{P\&O}$ is the P&O voltage step.

• SLG-Backstepping parameters:

$V_{inf} = 6V$, $\Delta V = 7V$, $\Delta P = 7W$, $K_1 = 1.3 \times 10^4$, $K_2 = 1.1 \times 10^4$.

• Resistive load:

$R = 50\Omega$, $P_{\max\_load} = 100W$.

With $P_{\max\_load}$ is the maximal power that can dissipate the resistive load used.

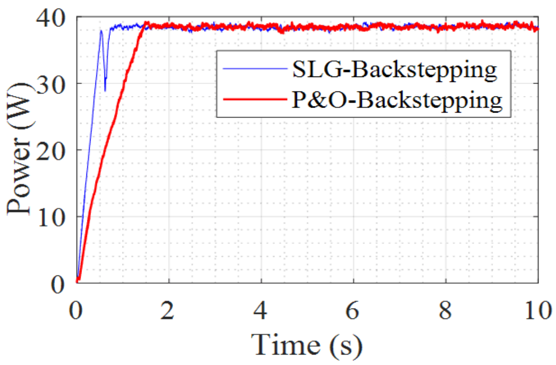

(a)

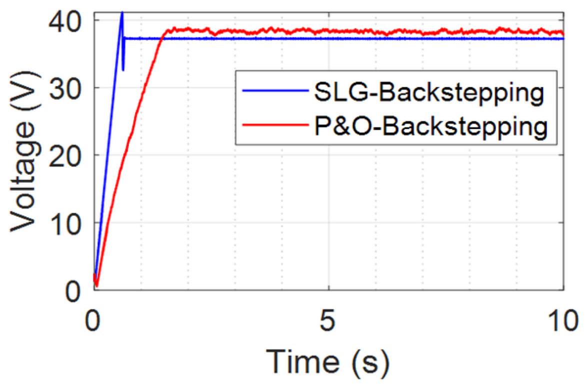

(b)

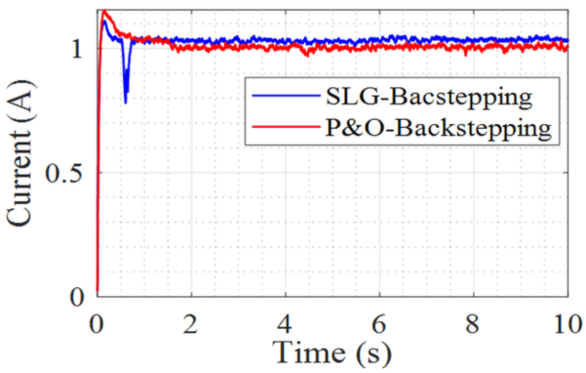

(c)

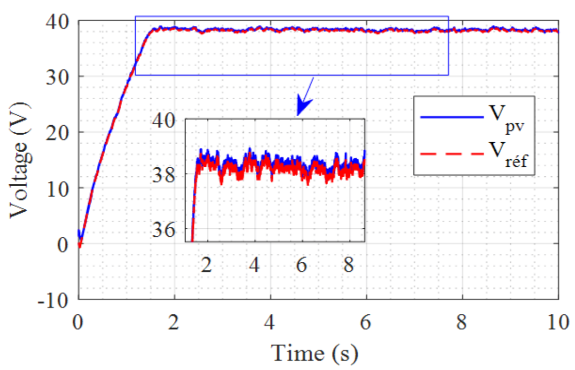

(d)

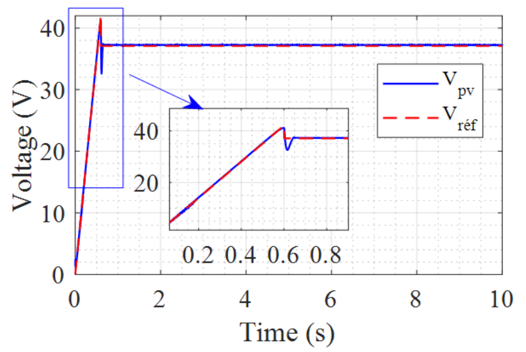

(e)

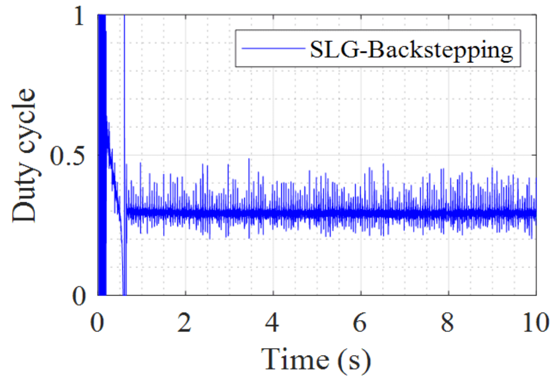

(f)

Fig. 6. Results obtained under uniform meteorological conditions. a - PV power, b - PV voltage, and c - PV current using the SLG-Backstepping and the P&O-Backstepping. d - PV voltage using the P&O-Backstepping technique. e - PV voltage, and f - Duty cycle using the SLG-Backstepping technique.

Initially, the photovoltaic modules are considered unshaded (under uniform meteorological conditions). Figure 6a illustrates the PV power produced using the P&O-Backstepping and SLG-Backstepping techniques. As can be seen in this figure, both techniques can reach the point of maximum power. Moreover, the proposed technique tracks the MPP faster than the P&O-Backstepping technique. The PV voltage, (see Fig.6b), produced using the P&O-Backstepping exhibits harmonics around its optimum as well as a significant rise-time. So, from these two figures, it can be concluded that the SLG algorithm offers tracking performances better than the P&O algorithm. In fact, based on the experimental data, the proposed SLG-Backstepping control strategy pursues GMPP in about 0.7s while P&O-Backstepping takes 1.5s to converge to the global maximum power point.

Figure. 6c depicts the PV current produced using both techniques discussed. While Fig.6f shows the control law (duty cycle) obtained using the SLG-Backstepping Command strategy.

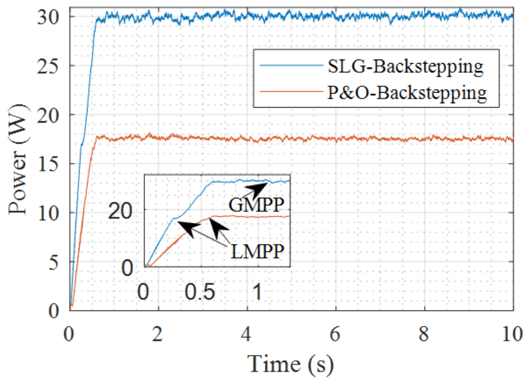

(a)

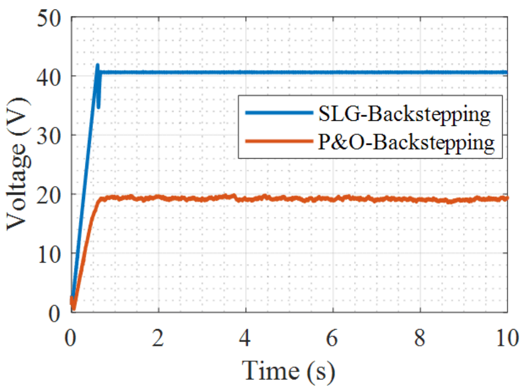

(b)

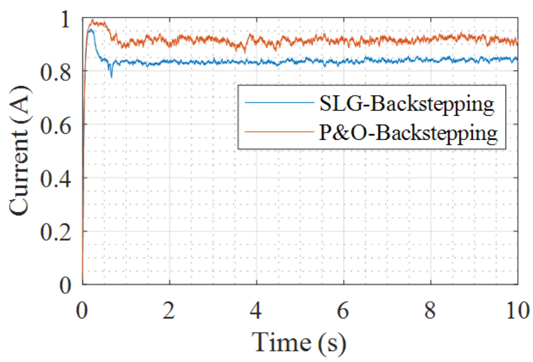

(c)

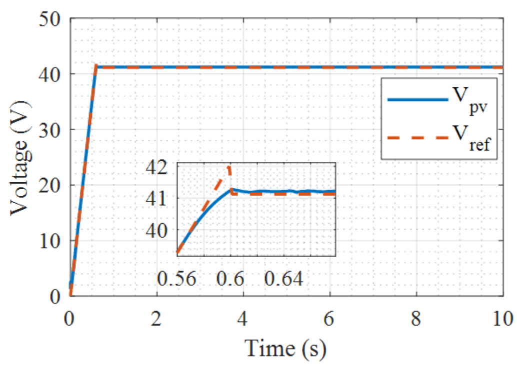

(d)

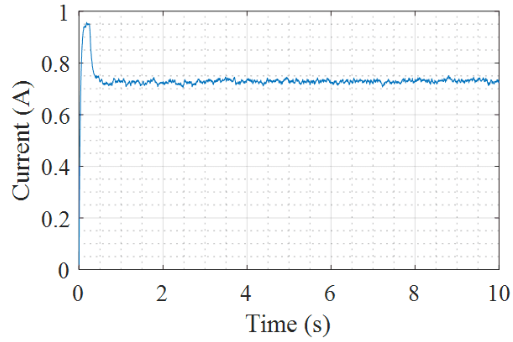

(e)

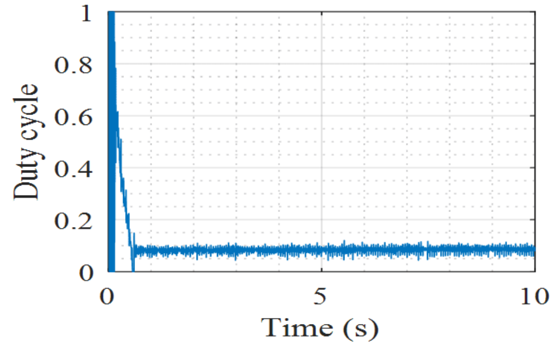

(f)

Fig. 7. Results obtained under partial shading effect. a - PV power, b – PV voltage, and c – PV current produced using the SLG-Backstepping and P&O-Backstepping techniques. d- PV voltage, e - PV current, and f - Duty cycle using proposed SLG-Backstepping technique.

Referring to Fig.6d and Fig.6e, it can be seen that the backstepping technique allows the Boost converter to quickly and accurately follow the voltage reference generated by the SLG or the P&O algorithm.

From now on, the PV modules are considered partially shaded as illustrated in Fig.1d. Under these conditions, the P-V curve can present one or two MPPs (one LMPP and one GMPP).

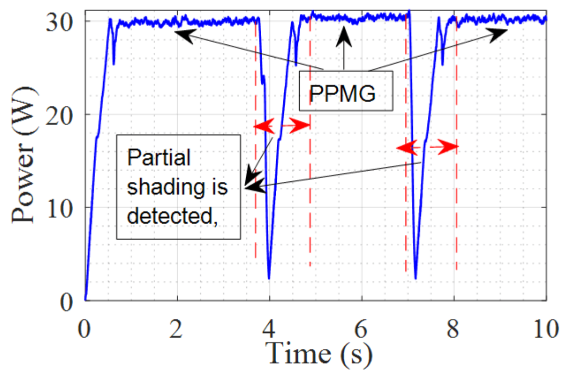

(a)

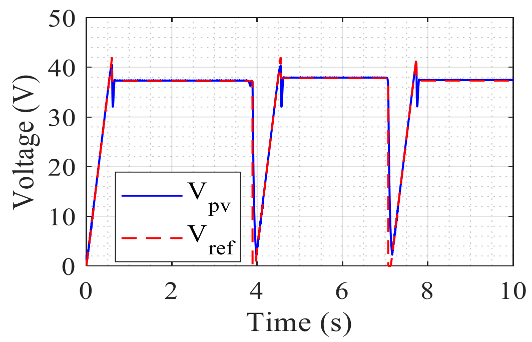

(b)

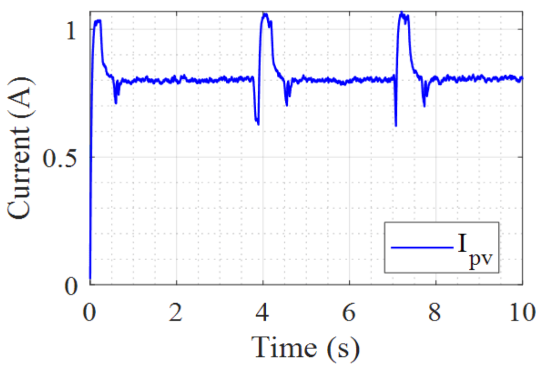

(c)

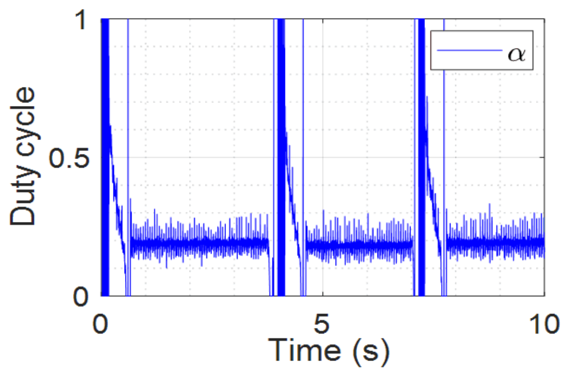

(d)

Fig. 8. Results obtained under temporary partial shading. a - PV power, b- PV voltage, c - PV current, and d - Duty cycle using the SLG-Backstepping technique.

Figure 7a, Fig.7b and Fig.7c respectively show the PV power, PV voltage and PV current produced using the P&O-Backstepping and the proposed SLG-Backstepping techniques. From Fig. 7a, it can be noted that the proposed technique has pursued the GMPP while the P&O-Backstepping has followed the LMPP. Thus, the MPPT techniques lead to considerable power losses in some cases. Indeed, based on experimental data, the P&O-Backstepping makes power losses of about 12W, these losses can be large in some cases depending on the shading pattern, while the GMPPT technique based on the proposed SLG-Backstepping conmmand strategy allows the PV system to extract the global maximum power point.

Figure 7d, Fig.7e and Fig.7f respectively illustrate the PV voltage, PV current and the duty cycle using the proposed technique.

Figure 8 shows the PV power, PV voltage, PV current and duty cycle obtained considering that the partial shading occurs instantly and disappears twice in a row. In this case, it can be seen that the proposed technique can rapidly locate and track the global maximum power point.

5. Conclusion

In this paper, the proposed SLG-Backstepping command strategy is implemented on the Arduino Mega 2560 Board. A Boost converter is designed in order to control the photovoltaic power and feed the resistive load in the real-time. The proposed technique is compared with the P&O-Backstepping under the partial shading and the uniform meteorological conditions, respectively. Indeed, the experimental tests have proven that the proposed technique can track the global maximum power point quickly and accurately in the real time, while the P&O-Backstepping technique results in a high-power loss under the partial shading effect. Furthermore, this technique is too slower compared to the proposed one under uniform meteorological conditions. Therefore, the proposed technique solves the issue of the partial shading and makes the photovoltaic sources more performants. Thus, it can be considered as a solution of power optimization for photovoltaic panels subjected to the non-uniform weather conditions (partially shaded photovoltaic panels).

References

[1] F. Lamzouri, E. Boufounas and A. El Amrani, "A Robust Backstepping Sliding Mode Control for MPPT based Photovoltaic System with a DC-DC Boost Converter", 2018 International Conference on Control, Automation and Diagnosis (ICCAD), Marrakech, Morocco, 2018.

[2] M. Mokhlis, M. Ferfra, A. Abbou, R. E. idrissi and C. C. Ahmed, "SMC based MPPT to track the GMPP under Partial Shading", 2019 7th International Renewable and Sustainable Energy Conference (IRSEC), Agadir, Morocco, pp. 1-6, 2019.

[3] S. Gautam, D. B. Raut, P. Neupane, D. P. Ghale and R. Dhakal, "Maximum power point tracker with solar prioritizer in photovoltaic application", 2016 IEEE International Conference on Renewable Energy Research and Applications (ICRERA), Birmingham, pp. 1051-1054, 2016.

[4] C. C. Ahmed, M. Cherkaoui and M. Mokhlis, "FL-SMC based MPPT for PV module Under uniform meteorological conditions", 2020 5th International Conference on Renewable Energies for Developing Countries (REDEC), Marrakech, Morocco, pp. 1-6, 2020.

[5] M. Mokhlis, M. Ferfra, H. A. Vall, R. E. idrissi, C. C. Ahmed and A. Taouni, "Design and Hardware Implementation of Backstepping Controller Dedicated to

the Photovoltaic Emulator", 2020 5th International Conference on Renewable Energies for Developing Countries (REDEC), Marrakech, Morocco, pp. 1-6, 2020.

[6] E. I. Rafika, A. Abbou, S. Rhaili and M. Salimi, "Maximum power point tracking of photovoltaic systems using backstepping controller", 2017 International Conference on Engineering and Technology (ICET), Antalya, pp. 1-6, 2017.

[7] M. Mokhlis, M. Ferfra, H. A. Vall, R. E. idrissi, C. C. Ahmed and A. Taouni, "Comparative Study Between the Different MPPT Techniques", 2020 5th International Conference on Renewable Energies for Developing Countries (REDEC), Marrakech, Morocco, pp. 1-6, 2020.

[8] D. Haji and N. Genc, "Fuzzy and P&O Based MPPT Controllers under Different Conditions", 2018 7th International Conference on Renewable Energy Research and Applications (ICRERA), Paris, pp. 649-655, 2018.

[9] M. Mokhlis, M. Ferfra, H. A. Vall, R. E. idrissi, C. C. Ahmed and A. Taouni, "Comparative Study Between the Different MPPT Techniques", 2020 5th International Conference on Renewable Energies for Developing Countries (REDEC), pp. 1-6, 2020.

[10] Abdelhakim BELKAIDa, Ilhami COLAK, Korhan KAYISLI and Ramazan BAYINDIR, "Design and Implementation of a Cuk Converter Controlled by a Direct Duty Cycle INC-MPPT in PV Battery System", International Journal of Smart Grid (ijSmartGrid), Vol.3, No.1, pp. 19-25, March 2019.

[11] D. Gueye, A. Ndiaye, M. Abdou Tankari, M. Faye, A. Thiam, L. Thiaw and G. Lefebvre, "Design Methodology of Novel PID for Efficient Integration of PV Power to Electrical Distributed Network", International Journal of Smart Grid (ijSmartGrid), Vol.2, No.1, pp. 77-86, March 2018.

[12] Mohcine Mokhlis, Mohammed Ferfra, "Optimization of Photovoltaic Panels Efficiency Using a Backstepping Control Technique Under Partial Shading Conditions", International Review on Modelling and Simulations (I.RE.MO.S), Vol. 10, No. 6, pp. 437-446, December 2017.

[13] P. Nagvekar and R. A. Metri, "An Improved GMPPT Technique Under Partial Shading Conditions for PV Array", 2019 International Conference on Computation of Power, Energy, Information and Communication (ICCPEIC), pp. 040-046, 2019.

[14] Mohcine Mokhlis, Mohammed Ferfra and Rafika El Idrissi, "High Gain Observer-Based Control for Grid-Connected PV System Under Partial Shading Effect", International Journal of Intelligent Engineering and Systems, Vol.13, No.2, pp. 161-172, 2020.

[15] M. Mokhlis, M. Ferfra and M. Chraygane, "Nonlinear Control of a Photovoltaic Pumping System under Partial Shading", 2017 International Renewable and Sustainable Energy Conference (IRSEC), Tangier, pp. 1-7, 2017.

[16] S. Marhraoui, A. Abbou, N. El Hichami, S. E. Rhaili and M. R. Tur, "Grid-Connected PV Using Sliding Mode Based on Incremental Conductance MPPT and VSC", 2019 8th International Conference on Renewable Energy Research and Applications (ICRERA), Brasov, Romania, pp. 516-520, 2019.

[17] E. i. Rafika, A. Abbou, M. Mohcine and M. Salimi, "A comparative study of MPPT controllers for photovoltaic pumping system", 2018 9th International Renewable Energy Congress (IREC), Hammamet, pp. 1-6, 2018.

[18] J. Wang, C. Wang, S. jia, S. Xiang and X. Shan, "Photovoltaic power MPPT controller based on fuzzy-backstepping method", 2019 8th International Symposium on Next Generation Electronics (ISNE), Zhengzhou, China, pp. 1-3, 2019.

[19] Muhammad Arsalan, Ramsha Iftikhar, Iftikhar Ahmad, Ammar Hasan, K. Sabahat, A. Javeria, "MPPT for photovoltaic system using nonlinear backstepping controller with integral action", Solar Energy, Vol. 170, pp. 192-200, August 2018.

[20] N. Skik and A. Abbou, "Robust adaptive integral backstepping control for MPPT and UPF of PV system connected to the grid", 2016 7th International Renewable Energy Congress (IREC), Hammamet, pp. 1-6, 2016.